Applied and Environmental Microbiology, July 2009, p. 4661–4667 Vol. 75, No. 14
0099-2240/09/$08.00+0 doi:10.1128/AEM.00409-09

Parasporal Body Formation via Overexpression of the Cry10Aa Toxin of *Bacillus thuringiensis* subsp. *israelensis*, and Cry10Aa-Cyt1Aa Synergism▽†

Alejandro Hernández-Soto,[1] M. Cristina Del Rincón-Castro,[2,3] Ana M. Espinoza,[1] and Jorge E. Ibarra[2]*

Centro de Investigación en Biología Celular y Molecular, Ciudad de la Investigación, Universidad de Costa Rica, San José, Costa Rica[1]; Departamento de Biotecnología y Bioquímica, CINVESTAV, Irapuato, Guanajuato, México[2]; and División de Ciencias de la Vida, Universidad de Guanajuato, Irapuato, Guanajuato, México[3]

Received 18 February 2009/Accepted 14 May 2009

***Bacillus thuringiensis* subsp. *israelensis* is the most widely used microbial control agent against mosquitoes and blackflies. Its insecticidal success is based on an arsenal of toxins, such as Cry4A, Cry4B, Cry11A, and Cyt1A, harbored in the parasporal crystal of the bacterium. A fifth toxin, Cry10Aa, is synthesized at very low levels; previous attempts to clone and express Cry10Aa were limited, and no parasporal body was formed. By using a new strategy, the whole Cry10A operon was cloned in the pSTAB vector, where both open reading frames ORF1 and ORF2 (and the gap between the two) were located, under the control of the *cyt1A* operon and the STAB-SD stabilizer sequence characteristic of this vector. Once the acrystalliferous mutant 4Q7 of *B. thuringiensis* subsp. *israelensis* was transformed with this construct, parasporal bodies were observed by phase-contrast microscopy and transmission electron microscopy. Discrete, ca. 0.9-μm amorphous parasporal bodies were observed in the mature sporangia, which were readily purified by gradient centrifugation once autolysis had occurred. Pure parasporal bodies showed two major bands of ca. 68 and 56 kDa on sodium dodecyl sulfate-polyacrylamide gel electrophoresis analysis. These bands were further characterized by N-terminal sequencing of tryptic fragments using matrix-assisted laser desorption ionization–time of flight mass spectrometry analysis, which identified both bands as the products of ORF1 and ORF2, respectively. Bioassays against fourth-instar larvae of *Aedes aegypti* of spore-crystal complex and pure crystals of Cry10Aa gave estimated 50% lethal concentrations of 2,061 ng/ml and 239 ng/ml, respectively. Additionally, synergism was clearly detected between Cry10A and Cyt1A, as the synergistic levels (potentiation rates) were estimated at 13.3 for the mixture of Cyt1A crystals and Cry10Aa spore-crystal complex and 12.6 for the combination of Cyt1A and Cry10Aa pure crystals.**

The subspecies *Bacillus thuringiensis* subsp. *israelensis* (serotype H-14) was discovered by Goldberg and Margalit in 1977 (11). To date, its insecticidal potential has not been overcome by any other bacterium (or any biological control agent) as an effective control measure against mosquito and blackfly larvae (8). Recently, its toxicity spectrum has been expanded to a coleopteran pest, the coffee berry borer (*Hypothenemus hampei*) (23), indicating that this strain may have potential versatility. Also, the so-called pBtoxis megaplasmid harbored in this strain, containing all the endotoxin-encoding genes found in its parasporal crystal, including *cry4A*, *cry4B*, *cry10A*, *cry11A*, and *cyt1A*, was recently sequenced (1). Among many other interesting aspects of this serotype, the occurrence of this mosquitocidal arsenal in one strain and their synergistic interaction make this bacterium scientifically and technologically attractive.

The parasporal crystal of *B. thuringiensis* subsp. *israelensis* contains large amounts of Cry4A, Cry4B, Cry11A, and Cyt1A toxins (14), and consequently, most of the knowledge about the toxicity of this strain has been focused on these proteins, acting either as a complex (31) or tested separately (6). Although the *cry10Aa* gene was originally cloned in 1986 (known then as *cryIVC*) (30), to date, little is known about *cry10Aa* and the protein it encodes, mostly due to its very low levels of expression (10) in *B. thuringiensis* subsp. *israelensis*. Interestingly, *cry10Aa* is an operon as it includes two open reading frames (ORFs), previously reported as pBt047 and pBt048 (hereafter referred to only as ORF1 and ORF2, respectively), separated by a 48-bp untranslated gap (1). ORF1 contains the complete δ-endotoxin sequence (active toxin), with a coding capacity for a 78-kDa protein. Interestingly, ORF2 shows high identity with the coding sequence of the C-terminal half of Cry4-type proteins, with a coding capacity for a 56-kDa protein. Therefore, it is believed that a putative ancestral *cry10Aa* gene is similar in size to the *cry4*-type genes (ca. 4 kbp), but either a small sequence had been inserted in the middle of the coding sequence or site mutations produced end codons (two end codons flank the gap) in this region (1).

Previous attempts to clone and express the *cry10Aa* gene included ORF1 and only part of ORF2 (7, 10, 30). This was a reasonable strategy, as most of the so-called "complete" protoxins are partially digested to become active toxins (δ-endotoxins) (28), and ORF1 included the complete sequence to code the Cry10Aa δ-endotoxin. However, in all these cases, the

* Corresponding author. Mailing address: CINVESTAV-IPN, Apartado Postal 629, 36500 Irapuato, Gto., Mexico. Phone: 52-462-623-9643. Fax: 52-462-624-5996. E-mail: jibarra@ira.cinvestav.mx.

† Supplemental material for this article may be found at http://aem.asm.org/.

▽ Published ahead of print on 22 May 2009.

expression levels were very low, and no parasporal body was formed. Similar results were obtained when the promoter was changed and a stabilizing sequence was added to the construction (13). The low expression levels achieved in these cases led to conclusions that assumed low toxic levels of Cry10Aa when tested against mosquito larvae (30). In spite of the low toxicity of Cry10Aa found against mosquito larvae, a synergistic effect was reported between Cry10Aa and Cry4Ba toxins in *Culex* (7). Obtaining high levels of expression and crystallization of Cry10Aa are required to properly characterize and understand the toxic spectrum of this protein.

In this report, we show the formation of parasporal bodies of Cry10Aa, achieved by cloning the whole Cry10Aa operon under the control of the *cyt1A* promoter and the STAB-SD sequence. We also show that Cry10Aa is as toxic as most of the other *B. thuringiensis* subsp. *israelensis* toxins acting separately, and in synergism with the Cyt1A toxin.

MATERIALS AND METHODS

Cloning of the Cry10Aa operon. In order to clone the complete sequence of the *cry10Aa* operon, which includes ORF1, ORF2, and the gap between the two (all in GenBank accession number AL731825), two primers were designed from the reported sequence (1). Sites for SalI and SphI were added to allow the subcloning of the amplicon into the pSTAB vector. The sequences of the designed primers were as follows: *cry*10D (direct), 5′-AATGTCGACTTGCAACAGAAAAGAGTTGTGTC-3′; and *cry*10R (reverse), 5′-CGAGCATGCACATTTCCCCACAATTTTCA-3′ (the SalI and SphI sites are underlined, respectively).

The *B. thuringiensis* subsp. *israelensis* strain ONR-60A, kindly provided by the International Entomopathogenic Bacillus Center at the Pasteur Institute, Paris, France, was subjected to DNA extraction following the protocol detailed by Jensen et al. (18). The PCR mixture comprised 500 ng template DNA, 12.5 μl double-distilled H_2O (ddH_2O), 2.5 μl of 10× reaction buffer, 2.5 μl of 225 mM $MgCl_2$, 0.5 μl deoxynucleoside triphosphate mixture, 20 μM of each primer, and 2.5 U *Taq* polymerase. A Perkin-Elmer GeneAmp PCR system 2400 thermocycler was set at the following conditions: an initial denaturation step of 5 min at 95°C, followed by 30 cycles, with 1 cycle consisting of denaturation at 95°C for 1 min, annealing at 50°C for 1.5 min, and polymerization at 70°C for 3 min. Amplification was completed with an extension step at 70°C for 10 min.

The expected 3,815-bp amplicon was cloned in the pCR2.1TOPO vector (Invitrogen) where, once ligated, it was used to transform competent *Escherichia coli* TOP-10 cells (Invitrogen) by thermoshock following the manufacturer's protocol. Transformed colonies were selected in plates with LB medium supplemented with 100 μg/ml ampicillin, 20 μg/ml 5-bromo-4-chloro-3-indolyl-β-D-galactopyranoside (X-Gal), and 100 μg/ml isopropyl-β-D-thiogalactopyranoside (IPTG). A set of 10 colonies was selected and subjected to plasmid extraction as described earlier (27), and the products were digested with EcoRV. The digestion products were visualized in 1% (wt/vol) agarose gels and compared to those obtained from the in silico analysis (BioEdit) (12) of the expected construct. This construct was called pCR2.1TOPO-*cry10*.

Both the pCR2.1TOPO-*cry10* construct and the pSTAB vector (kindly donated by B. Federici, University of California, Riverside, CA) (25) were digested with SalI and SphI, one enzyme at a time, and their products were visualized on and purified from agarose gels using the QIAquick gel extraction kit (Qiagen). Ligation of the 3,815-bp insert into the pSTAB vector at the specific SalI and SphI sites was carried out as previously described (27), and the new constructs were used to transform competent *E. coli* TOP-10 cells. Once transformed, colonies were selected and subjected to plasmid extraction. Single EcoRI and double EcoRI-SalI digestions were used to corroborate appropriate insertion of the *cry10Aa* operon into pSTAB. The new construct was called pSTAB-*cry*10.

This new construct was used to transform the acrystalliferous *B. thuringiensis* subsp. *israelensis* 4Q7 strain (kindly provided by the *Bacillus* Stock Center, Ohio State University, Columbus, OH) by electroporation following the protocol described by Lereclus et al. (20). Colonies selected in medium supplemented with 50 μg/ml erythromycin were subjected to plasmid purification (20), and the product was used as DNA template for the specific amplification of the *cry10Aa* gene. For this purpose, the following primers, described earlier (26), were used: 10A5 (direct) (5′-ATATGAAATATTCAATGCTC-3′) and 10A3 (reverse) (5′-ATAAATTCAAGTGCCAAGTA-3′). DNA from nontransformed 4Q7 strain was used as a negative control. Both the reaction mixture preparation and amplification conditions were as described above, except for the polymerization time, which was reduced to 1 min. Once the expected amplicon was obtained and purified, it was sequenced in an ABI PRISM 377 system (Applied Biosystems). The obtained sequence was analyzed by BlastN from the GenBank database.

Parasporal body formation. Once selected colonies of the *B. thuringiensis* subsp. *israelensis* 4Q7 strain transformed with the pSTAB-*cry*10 construct were obtained (Bt-pSTAB-*cry*10), they were inoculated in milk broth treated with peptone as previously described (15) to optimize the expression of the Cry10Aa protein. Cultures were monitored by phase-contrast microscopy until they reached the sporulation stage. Photographs were taken at a magnification of ×1,000. A more detailed visualization of the Bt-pSTAB-*cry*10 spore-crystal complex was obtained by transmission electron microscopy. For this purpose, mature sporangia were collected, washed, and fixed in 3% (vol/vol) glutaraldehyde in phosphate buffer (pH 7.4). Sporangia were sedimented in melted 2% (wt/vol) low-melting-point agarose to form an embedded pellet for further processing. The pellets were then dehydrated in an ethanol series and embedded in Spurr's low-viscosity resin mixture (Polysciences Inc.). Ultrathin sections were obtained with a NOVA LKB ultramicrotome and stained with lead citrate and uranyl acetate. Sections were examined and photographed in a Phillips Morgani electron microscope operated at an accelerating voltage of 80 kV.

Purification and sodium dodecyl sulfate-polyacrylamide gel electrophoresis (SDS-PAGE) analysis of parasporal bodies. Pure parasporal bodies from Bt-pSTAB-*cry*10 were obtained as previously described (14) by differential centrifugation in continuous NaBr gradients from an autolyzed culture obtained in milk broth treated with peptone. The band corresponding to the parasporal bodies was extracted and washed by centrifugation three times in ddH_2O. Parasporal bodies obtained from a 200-ml culture were suspended in 100 μl ddH_2O. A 20-μl aliquot was solubilized in a buffer containing 50 mM NaOH, 25 mM dithiothreitol, and 50 mM 3-(cyclohexylamino)-1-propanesulfonic acid (CAPS) (pH 11.5) and incubated for 1 h at 37°C. Then 10 μl of 4× Laemmli buffer [2% (wt/vol) SDS, 40% (vol/vol) glycerol, 5% (vol/vol) mercaptoethanol, 0.001% (wt/vol) bromophenol blue, 0.0625 M Tris-HCl (pH 8)] were added and incubated for 3 min in boiling water. Finally, 15 μl was loaded on a 10% (wt/vol) polyacrylamide gel and electrophoresed at 80 V for 4 h, basically by the method of Sambrook and Russell (27). The Bio-Rad 161-0304 molecular marker was used as a reference. Gels were stained in 0.25% (wt/vol) Coomassie brilliant blue, 40% (vol/vol) methanol, and 7% (vol/vol) acetic acid and destained in 40% (vol/vol) methanol and 7% (vol/vol) acetic acid.

Partial protein sequencing. Specific bands from polyacrylamide gels were sliced, taken out, and subjected to matrix-assisted laser desorption ionization–time of flight mass spectrometry (MALDI-TOF-MS) analysis as described previously (21) in order to obtain the partial amino acid sequences of several tryptic fragments from each band. The amino acid sequences obtained were subjected to Mascot Search analysis, and matches were analyzed individually with the BioEdit sequence analysis editor software (12).

In silico analysis of putative mRNAs from the Cry10Aa operon. Due to the limited or null expression of Cry10Aa in previous attempts (7, 13), an in silico analysis of the stability of the putative secondary structures of three possible mRNAs obtained from the operon was carried out. Previous attempts to express the Cry10Aa toxin used only ORF1 (and sometimes a fragment of ORF2). In this study, the stability of the secondary structure of the putative mRNA from the pSTAB-*cry*10 construct (ORF1-gap-ORF2) was compared with the putative mRNAs from each separate ORF using the RNAdraw v1.1 software (22).

Toxicological analysis. (i) Individual toxicity of Cry10Aa. Because the Cry10Aa toxin was expressed as a discrete inclusion body, an accurate toxicological analysis of its individual insecticidal activity could be performed. Bioassays on early fourth-instar larvae of *Aedes aegypti* were carried out essentially as previously described (17). Six to 10 concentrations of freeze-dried Bt-pSTAB-*cry*10 spore-crystal complex or Cry10Aa gradient-purified parasporal bodies were tested on each replicate. Twenty larvae, added to 100 ml dechlorinated water, were assayed per concentration along with a water-only negative control. A minimum of three replicates were carried out for each sample. Larvae were incubated at 28°C and examined after 24 h. The mean 50% lethal concentration (LC_{50}) was estimated for each preparation by probit analysis using the previously established statistical parameters (16).

(ii) Joint action of Cry10Aa and Cyt1Aa. Because a synergistic effect between the rest of the *B. thuringiensis* subsp. *israelensis* toxins has been well established (6, 29), a series of bioassays were performed in order to detect any synergistic effect between Cry10Aa and Cyt1Aa, which is the major synergistic component of the native parasporal body. The bioassay procedure was performed as described above. By using a freeze-dried powder of gradient-purified Cyt1Aa crys-

tals, an LC_{50} was estimated for this toxin acting alone. Then, by using 1:1 mixtures of Cyt1Aa crystals either with Bt-pSTAB-*cry*10 spore-crystal complex or with Cry10Aa gradient-purified crystals, an LC_{50} for each mixture was estimated. These estimates were then compared with the "expected" LC_{50} calculated using the formula reported by Tabashnik (29), which presumes an additive (nonsynergistic) joint action response between the tested factors. Synergism is inferred if the expected LC_{50} is greater than the highest fiducial limit ($P = 0.95$) of the experimentally estimated LC_{50}.

RESULTS

Cloning of the *cry10Aa* operon. A 3.8-kb amplification product was detected in agarose gels (see Fig. S1A in the supplemental material) after PCR amplification of ORF1 and ORF2 from the *cry10* operon using the *cry*10D and *cry*10R primers described in Materials and Methods. The corresponding 3,815-bp amplicon was cloned in the pCR2.1TOPO vector to constitute the new pCR2.1TOPO-*cry*10 construct, which was subjected to EcoRV digestion. As expected, 2.6-kb and 5.1-kb bands were detected by agarose electrophoresis (see Fig. S1B in the supplemental material), corresponding to a larger part of the insert and the vector with a fragment of the insert, respectively.

Once pCR2.1TOPO-*cry*10 was subjected to a double SalI-SphI digestion at the new sites added by the designed primers, the 3,815-bp insert was subcloned into the pSTAB vector by ligation at the corresponding SalI and SphI sites. The new construct, pSTAB-*cry*10, was subjected to single EcoRI and double EcoRI-SalI digestions, showing the expected 4.3-kb and 6.5-kb bands and 0.6-kb, 3.8-kb, and 6.5-kb bands, respectively, on electrophoretic analysis (see Fig. S1C in the supplemental material).

Next, pSTAB-*cry*10 was used to transform the acrystalliferous *B. thuringiensis* subsp. *israelensis* 4Q7 strain, and once selected, transformant colonies were subjected to DNA plasmid purification. When purified plasmids were used as templates to specifically amplify the *cry10Aa* gene with the previously reported 10A5 and 10A3 primers (26), a distinct ca. 550-bp band was obtained as a PCR product (see Fig. S1D in the supplemental material). The amplicon was sequenced, and its sequence was subjected to BlastN analysis, showing 100% identity with sequences corresponding to the *cry10Aa* gene previously reported (1, 30) (GenBank accession numbers AL731825.1 and M12662.1). No amplification was detected when DNA extracted from the nontransformed 4Q7 strain was used as a template.

Parasporal body formation. Once the *cry10* operon (ORF1-gap-ORF2) was cloned and transferred to the acrystalliferous 4Q7 strain, one transformant colony, called Bt-pSTAB-*cry*10, was selected for further analysis. First, this strain was observed by phase-contrast microscopy at the sporangium stage. Observations clearly indicated the formation of obvious parasporal bodies alongside the endospore (Fig. 1a). Parasporal bodies showed an amorphous semispherical shape, and it was common to observe two distinct inclusion bodies within each sporangium, one smaller than the other. These parasporal bodies were released during autolysis. As expected, nontransformed 4Q7 strain sporangia showed only endospores. Inclusion body formation was corroborated by transmission electron microscopy, where discrete parasporal bodies were clearly observed (Fig. 1b and c). Although crystallization of the recombinant protein was assumed in order to explain the formation of a discrete particle, lattice arrangement of molecules was not clear. Only a few limited areas of the inclusion bodies showed unclear paracrystalline arrangements of molecules. Furthermore, no defined shape of the inclusion body was observed, as it displayed diffused borders and scattered fragments, unlike the typical parasporal body of *B. thuringiensis* subsp. *israelensis*, where an envelope around the inclusion body is clearly observed. Still, the size of the recombinant parasporal body was somewhat similar to the native crystal, ranging from 0.57 to 0.92 μm, with an average of 0.75 μm at the longest axes.

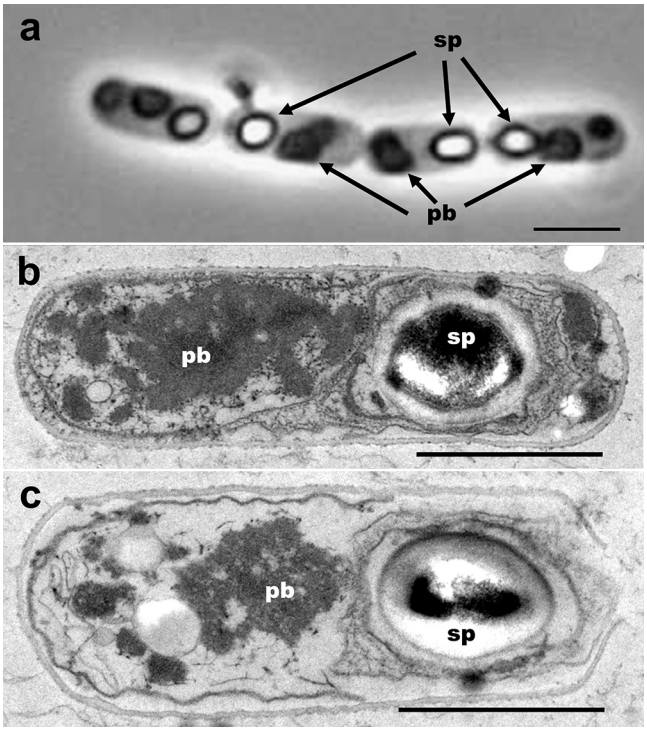

FIG. 1. Phase-contrast microscopy (a) and transmission electron microscopy (b) of mature sporangia (a and b) and sporangia close to autolysis (c) from the Bt-pSTAB-*cry*10 recombinant strain. sp, spore; pb, parasporal body. Bars, 2 μm (a) and 1 μm (b and c).

Purification and SDS-PAGE analysis of parasporal bodies. Autolyzed cultures of the Bt-pSTAB-*cry*10 strain were subjected to NaBr continuous gradient centrifugation. A distinctive band was formed at about two-thirds from the top of the tube (Fig. 2a), made up of >99% pure parasporal bodies as corroborated by phase-contrast microscopy. The pellet at the bottom of the gradient showed a mixture of spores and parasporal bodies. The protein composition of the purified parasporal crystals was analyzed by SDS-PAGE. For this purpose, pure crystals were washed, freeze-dried, dissolved in solubilization buffer (see Materials and Methods), and subjected to SDS-PAGE analysis. Pure crystals showed two major bands of ca. 68 kDa and 56 kDa and a minor band of ca. 78 kDa (Fig. 2b).

Partial protein sequencing. Precise identification of the major bands observed in the SDS-polyacrylamide gel was achieved by partial sequencing by MALDI-TOF-MS analysis. Each of the two major bands was excised from the gel and subjected to trypsin

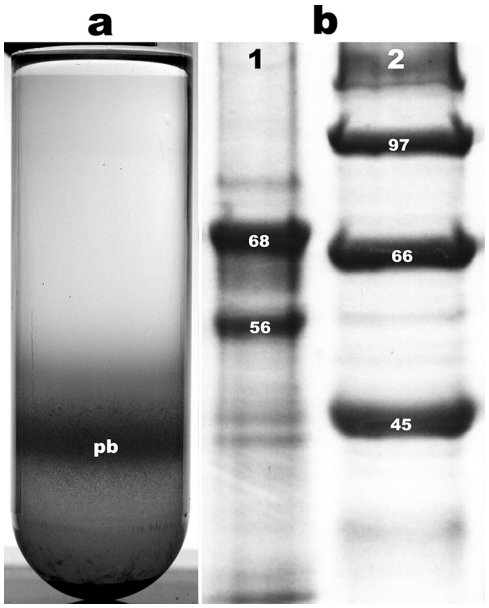

FIG. 2. (a) NaBr continuous gradient centrifugation of a Bt-pSTAB-*cry*10 recombinant strain autolyzed culture. pb, band containing the recombinant parasporal bodies. (b) SDS-PAGE analysis of gradient-purified Bt-pSTAB-*cry*10 recombinant strain parasporal bodies (lane 1) and molecular mass markers (lane 2). The numbers on the bands are the estimated molecular masses (in kilodaltons).

digestion. MALDI-TOF-MS sequence analysis of six and seven tryptic fragments from the ca. 68-kDa and 56-kDa bands, respectively, showed a perfect match with the amino acid sequences of the expected translations from Cry10Aa ORF1 and ORF2, respectively (GenBank accession numbers M12662.1 and CAD30099) (Table 1).

In silico analysis of putative mRNAs from the *cry10Aa* operon. According to the results obtained from the RNAdraw v1.1 software, a single mRNA that includes both ORF1 and ORF2 is 48% and 59% more stable at 37°C than separate mRNAs from ORF1 and ORF2, respectively. This may explain the success of cloning both ORFs in tandem in the expression of the Cry10Aa toxin.

Toxicity. (i) Individual toxicity of Cry10Aa. The mosquitocidal activity of the Cry10Aa toxin, expressed in strain Bt-pSTAB-*cry*10 acting alone, was estimated by bioassays against fourth-instar larvae of *Aedes aegypti*. For this purpose, both spore-crystal complexes and gradient-purified crystals were tested as freeze-dried powders. Once replicates fulfilled the minimal statistical requirements previously established (16), LC_{50}s of 2,061 ng/ml and 239 ng/ml were estimated when spore-crystal complexes and purified crystals, respectively, were tested (Table 2).

(ii) Joint action of Cry10Aa and Cyt1Aa. In order to test a possible synergism between the Cry10Aa toxin expressed in strain Bt-pSTAB-*cry*10 and the Cyt1Aa toxin, as previously found with other *B. thuringiensis* subsp. *israelensis* toxins (6, 29), a series of bioassays were conducted to test mixtures of pure Cyt1Aa crystals with either Bt-pSTAB-*cry*10 spore-crystal complexes or Cry10Aa pure parasporal bodies. Because synergism is established as a result of tests conducted first with the toxic factors acting separately and then acting together, an

TABLE 1. MALDI-TOF-MS sequences from tryptic fragments of the ca. 68-kDa and 56-kDa bands obtained from a polyacrylamide gel[a]

Band	Amino acid sequence of tryptic fragment	GenBank accession no. (gene)
68-kDa	SNNYSRYPLANKPNQPLK ELIREVYTNVNSDTFRTI TELENGLTR FPFYRNKPIDKVEIVR TDNYIFSVVR FLKNVSR IRYATNAPKTTVFLTGID TISVELPSTTSRONPNA TDLTYADFGYVTFPR	M12662.1 (ORF1 of *cry10Aa*)
56-kDa	LMLWDQVK GNYLNISGAR GFVGSSKDVELVVSR DVELVVSR QIVCQDSHQFK RSETQQAYVAK YLYDTR	CAD30099 (ORF2 of *cry10Aa*)

[a] Bands of ca. 68 kDa and 56 kDa were obtained from a polyacrylamide gel, when pure parasporal crystals from strain Bt-pSTAB-*cry*10 were electrophoresed.

LC_{50} of 739 ng/ml was estimated for pure Cyt1Aa crystals against fourth-instar larvae of *A. aegypti* (Table 2).

When a 1:1 mixture of the pure Cyt1Aa crystals and the Bt-pSTAB-*cry*10 spore-crystal complex was tested, an LC_{50} of 81.8 ng/ml was estimated. Likewise, when the same proportion was used for the pure Cyt1Aa and Cry10Aa parasporal bodies, an LC_{50} of 28.6 ng/ml was estimated. By using these data in the formula reported by Tabashnik (29), the expected LC_{50} for the joint action of the Cyt1Aa crystals and the spore-crystal complex was calculated to be 1,088 ng/ml if an additive (nonsynergistic) relationship between toxins was expected (Table 2). Likewise, the expected LC_{50} for the joint action of the Cyt1Aa and Cry10Aa purified parasporal bodies was calculated to be 362 ng/ml for an additive joint action response. When the expected and experimentally estimated LC_{50}s were compared, a clear synergistic effect was observed in both cases, with a synergistic level (potentiation rate) of 13.3 for the first combination and a potentiation rate of 12.6 for the second combination.

TABLE 2. Probit analysis data from the bioassays of the recombinant strain Bt-pSTAB-*cry*10 spore-crystal complex and pure crystals and their synergism with Cyt1Aa pure crystals against fourth-instar larvae of *Aedes aegypti*

Sample[a]	Exptl LC_{50} (FL) (ng/ml)[b]	Slope (±SE)	Expected LC_{50} (ng/ml)[c]
Cry10Aa s-c	2,061 (1,451–2,927)	1.05 (±0.15)	
Cry10Aa p-c	239 (182–312)	1.28 (±0.11)	
Cyt1Aa p-c	739 (630–866)	2.41 (±0.21)	
Cry10Aa s-c/Cyt1Aa p-c	81.8 (73.7–91.2)	3.49 (±0.31)	1,088
Cry10Aa p-c/Cyt1Aa p-c	28.6 (26.1–31.3)	4.46 (±0.46)	362

[a] s-c, spore-crystal complex; p-c, pure crystals; Cry10Aa s-c/Cyt1Aa p-c, combination of Cry10Aa s-c and Cyt1Aa p-c.

[b] LC_{50} (FL), lethal concentration causing 50% mortality and its fiducial limits at $P = 0.95$.

[c] Expected LC_{50} calculated by the method of Tabashnik (29).

DISCUSSION

Previous attempts to clone and express the *cry10Aa* gene from *B. thuringiensis* subsp. *israelensis* (7, 10, 13, 30) failed to achieve sufficient levels of expression to allow the formation of a parasporal inclusion body as usually occurs with most *B. thuringiensis* endotoxins. With the parasporal inclusion body formation achieved in this study, a precise toxicity level was estimated against mosquito larvae. Also, it was established that Cry10Aa acted synergistically with Cyt1Aa toxin, as occurs with the other endotoxins of *B. thuringiensis* subsp. *israelensis* (29).

The parasporal body formation of the Cry10Aa protein may be related to two factors. The first factor is the use of the pSTAB vector, which is under control of the *cyt1Aa* gene promoters and the STAB-SD stabilizer sequence from the *cry3A* gene just upstream of the coding sequence, in addition to a potential role of a modestly high vector copy number (ca. four), compared to the megaplasmid where the gene is originally harbored. This vector has been shown to increase up to 10 times the expression of other *cry* genes cloned under the control of these sequences (25). However, an earlier attempt to express the *cry10Aa* gene using this vector failed to form parasporal crystals (13), which might have been related to the cloning of only ORF1.

The second factor that can explain the high levels of expression obtained in this work is the cloning of the whole operon, including ORF1, ORF2, and the sequence between the two. A sequence analysis of ORF2 showed a high identity with the C-terminal halves of Cry4 toxins (3), indicating that *cry10Aa* may be the result of a natural mutation of a *cry4*-type gene which was truncated at approximately the middle of the gene (1, 9). Additionally, it has been proposed that, although the N-terminal halves of the toxins contain the δ-endotoxins (activated toxins), the C-terminal halves may have some effect on the crystallization of the protoxin (2, 28). If this is true, cloning both ORFs in tandem might explain the crystal formation in strain Bt-pSTAB-*cry*10. Other evidence that may support this hypothesis is the analysis of the secondary structure stability of the putative mRNAs from separate ORF1 and ORF2 and a single mRNA from the whole operon, the latter being significantly more stable. However, taking into account the facts that the entire Cry10A operon is present in the wild-type strain and its expression levels are still very low (10), expression competence among the other endotoxin genes in the wild-type strain should also be considered. Therefore, the expression levels observed in this work may be the effect of a combination of factors: the vector (more precisely, the *cyt1A* promoter and the STAB-SD sequence), the cloning of the whole operon, and the lack of expression competence in the recombinant strain.

It is important to note that the occurrence of this type of arrangement among the *cry* genes (ORF1-gap-ORF2), where ORF2 shows high identity with the C-terminal halves of so-called "complete" endotoxins, is found in some other instances, such as *cry30A*, *cry30B*, *cry30C*, *cry39Aa*, and *cry40Aa* (9; *Bacillus thuringiensis* toxin nomenclature website http://www.lifesci.sussex.ac.uk/Home/Neil_Crickmore/Bt/). More interesting is the high identity shown by the gaps between the two ORFs in all these cases. Excluding *cry30A*, a Kimura analysis (19) of these gaps showed an average genetic distance of 0.2, indicating a possible common origin. The results obtained in this research may be the basis to explore how the expression of these other *cry* genes may be affected if both ORFs are cloned in tandem using a powerful regulating sequence.

Parasporal bodies observed in the recombinant strain Bt-pSTAB-*cry*10 showed an amorphous, sometimes semispherical, inclusion body and an additional smaller fragment within the same sporangium. Both inclusion bodies may be the result of a separate crystallization process of each protein expressed from each ORF, as they were also detected separately in the SDS-PAGE analysis. However, more detailed studies are required to prove this, as both large and small inclusion bodies may be made up of a mixture of both proteins. In fact, this might be the reason why these crystals were so difficult to solubilize, as a special buffer was necessary to achieve solubilization (see Materials and Methods). It is known that the typical *B. thuringiensis* subsp. *israelensis* parasporal inclusion body is made up of three protoxins, Cry4A, Cry4B, and Cyt1A, whereas Cry11A is formed slightly separated in a bar-shaped inclusion body (14). Also, the typical bipyramidal crystals of lepidopteran-active protoxins of *B. thuringiensis* are frequently made up of a homogeneous blend of Cry1-type proteins (4, 32). In spite of its seemingly low density, the size of the Bt-pSTAB-*cry*10 parasporal body is somewhat similar to the sizes of most *B. thuringiensis* crystals (28), which indicates a normal expression level of the protein. However, the native *cry10Aa* gene is normally expressed in such low levels in *B. thuringiensis* subsp. *israelensis* that its detection as part of the crystal or in polyacrylamide gels is very difficult (10).

It is worth noting that actual crystallization (lattice formation) of the recombinant proteins were not clearly observed by transmission electron microscopy. The parasporal bodies showed a more diffuse and loose structure, rather than a compact particle, but could still be purified by differential centrifugation. Nevertheless, it is worth mentioning that observation of a lattice by transmission electron microscopy of *B. thuringiensis* crystals is very unusual, and in the case of *B. thuringiensis* subsp. *israelensis*, a lattice has been observed only in the attached bar-shaped inclusion body formed by Cry11A proteins (14). Another feature typical of the native *B. thuringiensis* subsp. *israelensis* crystal, which is missing in the recombinant Cry10Aa parasporal body, is the surrounding envelope that keeps the different observed inclusion bodies together. However, a loose envelope was usually observed around the recombinant parasporal bodies, which might be either part of the mother cell wall or a projection of the exosporium (Fig. 1b and c). Scanning electron microscopy analysis of the recombinant parasporal bodies might have helped to resolve their particulate nature. Unfortunately, several attempts to do this resulted in ambiguous and inconsistent observations that made it difficult to draw sound conclusions.

As mentioned above, SDS-PAGE analysis of the pure Cry10Aa parasporal bodies revealed that ORF1 and ORF2 were being translated effectively and separately, as two major bands (ca. 68 kDa and 56 kDa) appeared on the gel. The expected molecular mass for the translated ORF2 was precisely 56.3 kDa, which matches the bottom band in the gels and with the partial amino acid sequences from its tryptic fragments. However, the expected molecular mass of the translated ORF1 is 77.8 kDa, almost a 10-kDa difference from the observed top band in the gels in spite of its perfect match with

the partial amino acid sequences from its tryptic fragments. Perhaps the original expression product is being processed either postranscriptionally or postranslationally, or it is simply degraded to a smaller protein. According to MALDI-TOF-MS analysis, there must be a loss of the 22 N-terminal residues and the 63 C-terminal residues to leave a 67.9-kDa protein which matches the observed band. Degradation of the original protein may be the most feasible reason, as there are reports indicating that this phenomenon occurs in other Cry proteins (5, 24), although its insecticidal activity remains in this fragment. Removal of N-terminal residues during activation of the protoxin into the δ-endotoxin is common in most Cry proteins. Also it is worth noting the following: first, that polyacrylamide gels showed a minor band of ca. 78 kDa (Fig. 2b), which may correspond to the undegraded product from ORF1; and second, that both of these two expression products are very different from the 58-kDa protein reported earlier as Cry10Aa (10). Additionally, the fact that ORF2 is translated separately from ORF1 may indicate that a putative ancestral Cry4-type gene was subdivided, but some kind of adaptive benefit selected for reactivation of the nontoxic part of the gene.

The complex toxin arsenal of *B. thuringiensis* subsp. *israelensis* (6, 30) makes it difficult to assess the contribution of each component by testing them separately. Still, it has been possible to test individual contributions of Cry4A, Cry4B, Cry11A, and Cyt1A (6) and their synergistic interactions. Individual toxicity of Cry10A has been tested under considerable limitations (7, 30), as no parasporal bodies had been obtained before, leading to erroneous conclusions on its low toxicity (7, 13). Inclusion body formation of this toxin made it possible to obtain a precise toxicity level and, even more significantly, to prove its synergistic interaction with the Cyt1A toxin. Interestingly and in contrast to previous reports (10, 30), the toxicity level of Cry10A acting individually is similar to that observed with other Cry proteins from *B. thuringiensis* subsp. *israelensis* (6). It should also be pointed out that the toxicity estimated for Cyt1Aa acting alone was comparable to the toxicity in previous reports (6), with an LC_{50} 1.6 times lower than previously estimated.

Based on the difference between the LC_{50}s estimated for the Bt-pSTAB-*cry*10 spore-crystal complex and the pure crystals, much of the spore-crystal complex consists of spores and cell debris (85 to 88%). Still, in spite of the great difference in toxicity between these two preparations, the synergistic levels (potentiation rates) are about the same (13.3 and 12.6, respectively), which should be expected as the potentiation rate is independent of the concentration of each tested factor. While the toxicity of pure crystals should be higher than the toxicity of spore-crystal complex (as it occurred), potentiation rates should remain similar, as these only indicate the level of synergism in the mixture. Interestingly, when potentiation rates were calculated from data reported previously (6, 29), they were comparable only with those observed between Cry4-type toxins and Cyt1Aa, that is, the highest potentiation rates obtained so far. These results may suggest that if Cry10Aa were expressed at higher levels in the wild-type strain, its toxicity may be significantly increased. Also, in the case of a possible development of resistance to the wild-type strain by mosquito larvae (a situation that has not occurred up till now), the overexpression of Cry10Aa in the wild-type strain may be considered a control alterative. However, it is worth noting that even if the expression level of Cry10Aa observed in strain Bt-pSTAB-*cry*10 ensures the formation of parasporal bodies, the yield in terms of total biomass is low, as most of the dry weight is made up of spores and cell debris (see above). Also, the low growth rate of the recombinant strain that was observed may be due to the presence of erythromycin in the medium, as its elimination restores the normal growth rate.

In conclusion, parasporal body formation was achieved from a relatively unknown toxin of *B. thuringiensis* subsp. *israelensis*. Its toxicity is comparable to the other toxins in this serotype, and like those, it also shows synergism with the Cyt1A toxin. The potential of Cry10Aa is high and must be added to the arsenal of mosquitocidal toxins from *B. thuringiensis*. The results reported here may form the basis for novel approaches to delaying potential insect resistance, increasing the toxicity of the wild-type strain, studying the complex toxin interaction in this strain, and broadening the toxic spectrum toward other insect species.

ACKNOWLEDGMENTS

We thank Regina Basurto, Javier Luévano, Aurora Verver, Lourdes Palma, and Alicia Chagolla for their excellent technical support. We also thank the Institut Pasteur and B. Federici for providing key materials.

This project was partially supported by the United Nations University/BIOLAC (Venezuela), CYTED project III.5 (Spain), the Ministry of Foreign Affaires (SRE/PMCID, Mexico), and CONACYT (Mexico).

REFERENCES

1. **Berry, C., S. O'Neil, E. Ben-Dov, A. F. Jones, L. Murphy, M. A. Quail, M. T. G. Holden, D. Harris, A. Zaritsky, and J. Parkhill.** 2002. Complete sequence and organization of pBtoxis, the toxin-coding plasmid of *Bacillus thuringiensis* subsp. *israelensis*. Appl. Environ. Microbiol. **68:**5082–5095.
2. **Bietlot, H., I. Vishnubhatla, R. Carey, M. Pozsgay, and H. Kaplan.** 1990. Characterization of the cysteine residues and disulfide linkages in the protein crystal of *Bacillus thuringiensis*. Biochem. J. **267:**309–316.
3. **Bravo, A.** 1997. Phylogenetic relationships of *Bacillus thuringiensis* δ-endotoxin family proteins and their functional domains. J. Bacteriol. **179:**2793–2801.
4. **Bulla, L., K. Kramer, and L. Davidson.** 1977. Characterization of the entomocidal parasporal crystal of *Bacillus thuringiensis*. J. Bacteriol. **130:**375–383.
5. **Chilcott, C. N., J. Kalmakoff, and J. S. Pillai.** 1983. Characterization of proteolytic activity associated with *Bacillus thuringiensis* var. israelensis crystals. FEMS Microbiol. Lett. **18:**37–41.
6. **Crickmore, N., E. J. Bone, J. A. Williams, and D. Ellar.** 1995. Contribution of the individual components of the δ-endotoxin crystal to the mosquitocidal activity of *Bacillus thuringiensis* subsp. *israelensis*. FEMS Microbiol. Lett. **131:**249–254.
7. **Delécluse, A., C. Bourgouin, A. Klier, and G. Rapoport.** 1988. Specificity of action on mosquito larvae of *Bacillus thuringiensis israelensis* toxins encoded by two different genes. Mol. Gen. Genet. **214:**42–47.
8. **Delécluse, A., V. Juárez-Pérez, and C. Berry.** 2000. Vector-active toxins: structure and diversity, p. 101–125. *In* J. F. Charles, A. Delecluse, and C. Nielsen-LeRoux (ed.), Entomopathogenic bacteria: from laboratory to field application. Kluwer Academic Publishers, Dordrecht, The Netherlands.
9. **de Maagd, R., A. Bravo, C. Berry, N. Crickmore, and E. Schnepf.** 2003. Structure, diversity and evolution of protein toxins from spore forming entomopathogenic bacteria. Annu. Rev. Genet. **37:**409–433.
10. **Garduno, F., L. Thorne, A. Walfield, and T. Pollock.** 1988. Structural relatedness between mosquitocidal endotoxins of *Bacillus thuringiensis* subsp. *israelensis*. Appl. Environ. Microbiol. **54:**277–279.
11. **Goldberg, L. J., and J. Margalit.** 1977. A bacterial spore demonstrating rapid larvicidal activity against *Anopheles sergentii*, *Uranotaenia unguiculata*, *Culex univitattus*, *Aedes aegypti* and *Culex pipiens*. Mosq. News **37:**355–358.
12. **Hall, T. A.** 1999. BioEdit: a user-friendly biological sequence alignment editor and analysis program for Windows 95/98/NT. Nucleic Acids Symp. Ser. **41:**95–98.
13. **Hughes, P., M. Stevens, H. Park, B. Federici, E. Dennis, and R. Akhurst.** 2005. Response of larval *Chironomus tepperi* (Diptera: Chironomidae) to individual *Bacillus thuringiensis* var. *israelensis* toxins and toxin mixtures. J. Invertebr. Pathol. **88:**34–39.

14. **Ibarra, J. E., and B. A. Federici.** 1986. Isolation of a relatively nontoxic 65-kilodalton protein's inclusion from the parasporal body of *Bacillus thuringiensis* subsp. *israelensis*. J. Bacteriol. **165:**527–533.
15. **Ibarra, J. E., and B. A. Federici.** 1986. Parasporal bodies of *Bacillus thuringiensis* subsp. *morrisoni* (PG-14) and *Bacillus thuringiensis* subsp. *israelensis* are similar in protein composition and toxicity. FEMS Microbiol. Lett. **34:** 79–84.
16. **Ibarra, J. E., and B. A. Federici.** 1987. An alternative bioassay for determining the toxicity of suspended particles to mosquito larvae. J. Am. Mosq. Control Assoc. **3:**187–192.
17. **Ibarra, J. E., M. C. del Rincon, S. Orduz, D. Noriega, G. Benintende, R. Monnerat, L. Regis, C. M. F. de Oliveira, H. Lanz, M. H. Rodriguez, J. Sanchez, G. Pena, and A. Bravo.** 2003. Diversity of *Bacillus thuringiensis* strains from Latin America with insecticidal activity against different mosquito species. Appl. Environ. Microbiol. **69:**5269–5274.
18. **Jensen, G., A. Wilkins, S. Petersen, J. Damgaard, J. Baum, and L. Andrup.** 1995. The genetic basis of the aggregation system in *Bacillus thuringiensis* subsp. *israelensis* is located on the large conjugative plasmid pX016. J. Bacteriol. **17:**2914–2917.
19. **Kimura, M.** 1980. A simple model for estimating evolutionary rates of base substitutions through comparative studies of nucleotide sequences. J. Mol. Evol. **16:**111–120.
20. **Lereclus, D., O. Arantes, J. Chaufax, and M. Lecadet.** 1989. Transformation and expression of a cloned δ-endotoxin gene in *Bacillus thuringiensis*. FEMS Microbiol. Lett. **60:**211–218.
21. **López, M. G., N. A. Mancilla-Margalli, and G. Mendoza-Diaz.** 2003. Molecular structures of fructans from *Agave tequilana* Weber var. azul. J. Agric. Food Chem. **51:**7835–7840.
22. **Matzura, O., and A. Wennborg.** 1996. RNAdraw: an integrated program for RNA secondary structure calculation and analysis under 32-bit Microsoft Windows. Bioinformatics **12:**247–249.
23. **Méndez-López, I., R. Basurto, and J. E. Ibarra.** 2003. *Bacillus thuringiensis* serovar *israelensis* is highly toxic to the coffee berry borer, *Hyphotenemus hampei* Ferr. (Coleoptera: Scolytidae). FEMS Microbiol. Lett. **226:**73–76.
24. **Oppert, B.** 1999. Protease interactions with *Bacillus thuringiensis* insecticidal toxins. Arch. Insect Biochem. Physiol. **42:**1–12.
25. **Park, H.-W., B. Ge, L. S. Bauer, and B. A. Federici.** 1998. Optimization of Cry3A yields in *Bacillus thuringiensis* by use of sporulation-dependent promoters in combination with the STAB-SD mRNA sequence. Appl. Environ. Microbiol. **64:**3932–3938.
26. **Porcar, M., and V. Juárez-Pérez.** 2003. PCR-based identification of *Bacillus thuringiensis* pesticidal crystal genes. FEMS Microbiol. Rev. **26:**419–432.
27. **Sambrook, J., and D. W. Russell.** 2001. Molecular cloning: a laboratory manual, 3rd ed. Cold Spring Harbor Laboratory Press, Cold Spring Harbor, NY.
28. **Schnepf, E., N. Crickmore, J. Van Rie, D. Lereclus, J. Baum, J. Feitelson, D. R. Zeigler, and D. H. Dean.** 1998. *Bacillus thuringiensis* and its pesticidal proteins. Microbiol. Mol. Biol. Rev. **68:**775–806.
29. **Tabashnik, B. E.** 1992. Evaluation of synergism among *Bacillus thuringiensis* toxins. Appl. Environ. Microbiol. **58:**3343–3346.
30. **Thorne, L., F. Garduno, T. Thompson, D. Decker, M. Zounes, M. Wild, A. Walfield, and T. Pollock.** 1986. Structural similarity between the lepidoptera- and diptera-specific insecticidal endotoxin genes of *Bacillus thuringiensis* subsp. "kurstaki" and "*israelensis*." J. Bacteriol. **166:**801–811.
31. **Tyrell, D. J., L. I. Davidson, L. A. Bulla, Jr., and W. A. Ramoska.** 1979. Toxicity of parasporal crystals of *Bacillus thuringiensis* subsp. *israelensis* to mosquitoes. Appl. Environ. Microbiol. **38:**656–658.
32. **Tyrell, D. J., L. Bulla, R. Andrews, K. Kramer, L. Davidson, and P. Nordin.** 1981. Comparative biochemistry of entomocidal parasporal crystals of selected *Bacillus thuringiensis* strains. J. Bacteriol. **145:**1052–1062.